iScience

CellPress
OPEN ACCESS

Article

Neuroepithelial cell-transforming 1 promotes cardiac fibrosis via the Wnt/β-catenin signaling pathway

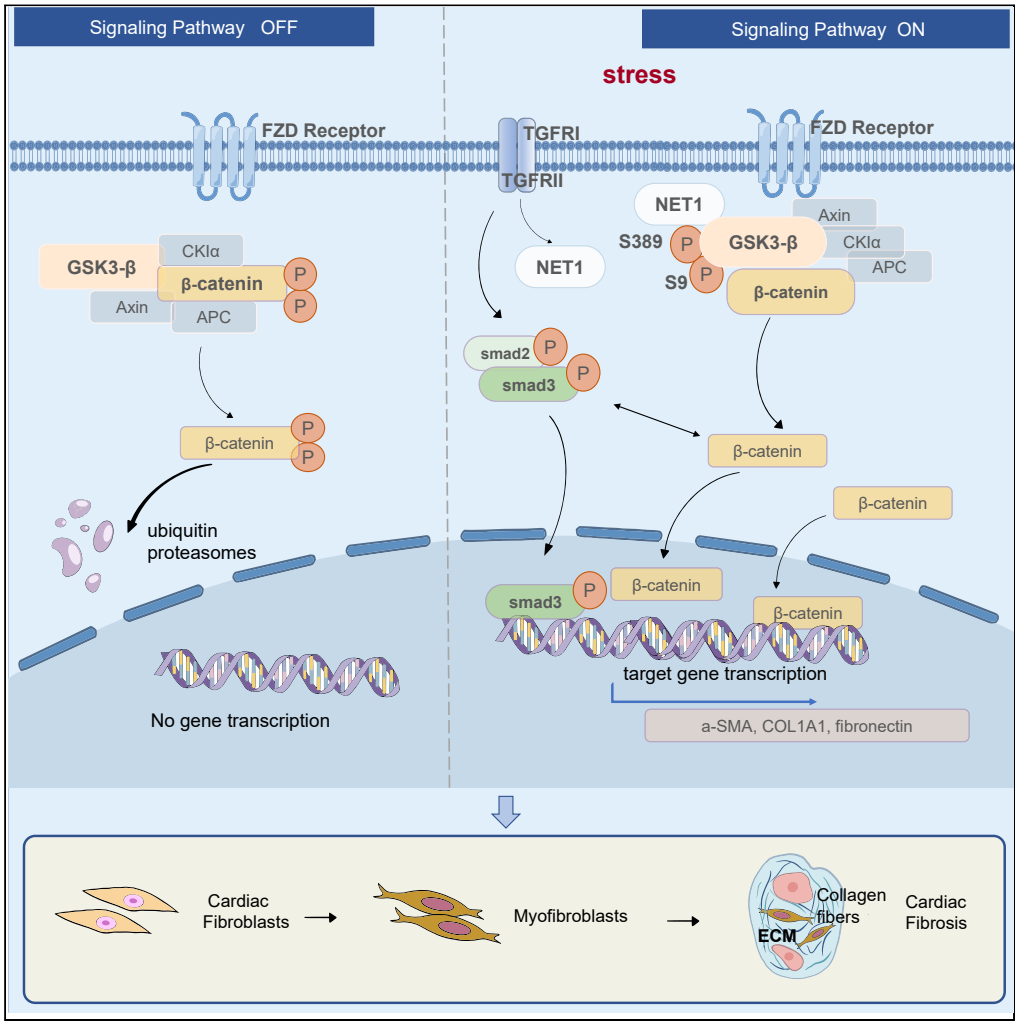

Tianyu Li, Xue Xiong, Yujing Wang, ..., Haihai Liang, Xuelian Li, Hongli Shan

lixuelian@hrbmu.edu.cn (X.L.)
shanhl@sues.edu.cn (H.S.)

Highlights

The expression level of NET1 was significantly increased *in vivo* and *in vitro*

Overexpression of NET1 may form a complex with β-catenin through GSK3β

NET1 participated in cardiac fibrosis by acting on Wnt/β-catenin and TGF-β pathway

Li et al., iScience *26*, 107888
October 20, 2023
https://doi.org/10.1016/j.isci.2023.107888

iScience

CellPress
OPEN ACCESS

Article

Neuroepithelial cell-transforming 1 promotes cardiac fibrosis via the Wnt/β-catenin signaling pathway

Tianyu Li,[1,6,7] Xue Xiong,[1,7] Yujing Wang,[1,7] Yue Li,[1,7] Yao Liu,[1] Mingxiu Zhang,[1] Chao Li,[1] Tong Yu,[2] Wei Cao,[3] Shuangshuang Chen,[1] Huizhen Zhang,[1] Xiaona Wang,[1] Lifang Lv,[4] Yuhong Zhou,[1] Haihai Liang,[1,5] Xuelian Li,[1,8,*] and Hongli Shan[1,2,*]

SUMMARY

This study found that the level of neuroepithelial cell-transforming gene 1 protein (NET1) was significantly increased in a mouse cardiac fibrosis model. Moreover, the expression level of NET1 was increased in cardiac fibrosis induced by TGF-β1, suggesting that NET1 was involved in the pathological process of cardiac fibrosis. Overexpression of NET1 promoted β-catenin expression in the nucleus and significantly increased the proliferation and migration of cardiac fibroblasts. NET1 may form a complex with β-catenin through GSK3β. Knockdown of β-catenin alleviated the effects of NET1 overexpression on collagen production and cell migration. In the heart of NET1 knockout mice, NET1 knockout can reduce the expression of β-catenin, α-SMA, and collagen content induced by MI. In conclusion, NET1 may regulate the activation of Wnt/β-catenin and TGF/Smads signaling pathway, promote collagen synthesis in fibroblasts, and participate in cardiac fibrosis. Thus, NET1 may be a potential therapeutic target in cardiac fibrosis.

INTRODUCTION

Cardiac fibrosis is one of the primary features of many acute and chronic heart diseases and is characterized by cell proliferation, excessive deposition of extracellular matrix proteins, excessive accumulation of collagen fibers, a significant increase in collagen concentration, and changes in collagen composition. Its main pathological manifestations include increased myocardial stiffness, decreased myocardial contractility, decreased coronary flow reserve, malignant arrhythmia, and sudden death.[1,2]

Neuroepithelial cell transforming 1 is a member of the guanine nucleotide exchange factor (GEF) family that activates and regulates Rho family members by catalyzing the conversion of guanosine diphosphate to guanosine triphosphate. NET1 can regulate the activity of RhoA in two ways. First, NET1 regulates the binding of GTP and RhoA proteins through the DH-PH domain, thereby regulating the activity of RhoA protein.[3] Second, NET1 can interact with Dlg1 protein through the PDZ domain, preventing its proteasomal degradation, and significantly promotes the activity of RhoA to regulate intercellular signal transduction.[4] Application of Rho inhibitor or mut-NET1 significantly inhibits cell viability of SC-4 epithelial cells and its epithelial-mesenchymal transition (EMT), suggesting that NET1 and Rho signals are critical in this process. NET1 promotes the proliferation and migration of mouse embryonic fibroblast (NIH3T3) cells.[5] A 2017 study of GEFs highlighted the importance of RhoA as a pro-fibrotic signaling pathway in idiopathic pulmonary fibrosis. These findings suggest that NET1 may be involved in the pathogenesis of cardiac fibrosis. However, whether NET1 is definitively involved in cardiac fibrosis has not been reported.

In our previous experiment using mouse models of TAC-induced pressure overload cardiac fibrosis or ischemic myocardial infarction (MI), we found a significantly increased expression of NET1 in the myocardium of these mice lasting 8 weeks or for 7 days, respectively, confirming the expression of NET1 in the heart. Therefore, NET1 may play a key role in the process of cardiac fibrosis, but the specific mechanism needs to be further explored. Activation of the Wnt/β-catenin signaling pathway in zebrafish embryos requires NET1, which can activate dimerized PAK1. Further phosphorylation of the S675 site of β-catenin induces transcriptional activity of signaling molecules downstream of β-catenin.[6] This result suggests NET1 may be related to the Wnt/β-catenin pathway, which is an important pathway in cardiac fibrosis pathology.

[1]Department of Pharmacology (State-Province Key Laboratories of Biomedicine-Pharmaceutics of China, Key Laboratory of Cardiovascular Research, Ministry of Education), College of Pharmacy, Harbin Medical University, Harbin, Heilongjiang 150081, P.R. China
[2]Shanghai Frontiers Science Research Center for Druggability of Cardiovascular Noncoding RNA, Institute for Frontier Medical Technology, Shanghai University of Engineering Science, Shanghai 201620, P.R. China
[3]Department of Cardiology, The Second Affiliated Hospital of Harbin Medical University, Harbin, Heilongjiang 150086, P.R. China
[4]The Centre of Functional Experiment Teaching, School of Basic Medicine, Harbin Medical University, Harbin, Heilongjiang 150081, P.R. China
[5]Research Unit of Noninfectious Chronic Diseases in Frigid Zone (2019RU070), Chinese Academy of Medical Sciences, Harbin 150081, P.R. China
[6]Heilongjiang University of Chinese Medicine, Harbin, Heilongjiang 150040, P.R. China
[7]These authors contributed equally
[8]Lead contact
*Correspondence: lixuelian@hrbmu.edu.cn (X.L.), shanhl@sues.edu.cn (H.S.)
https://doi.org/10.1016/j.isci.2023.107888

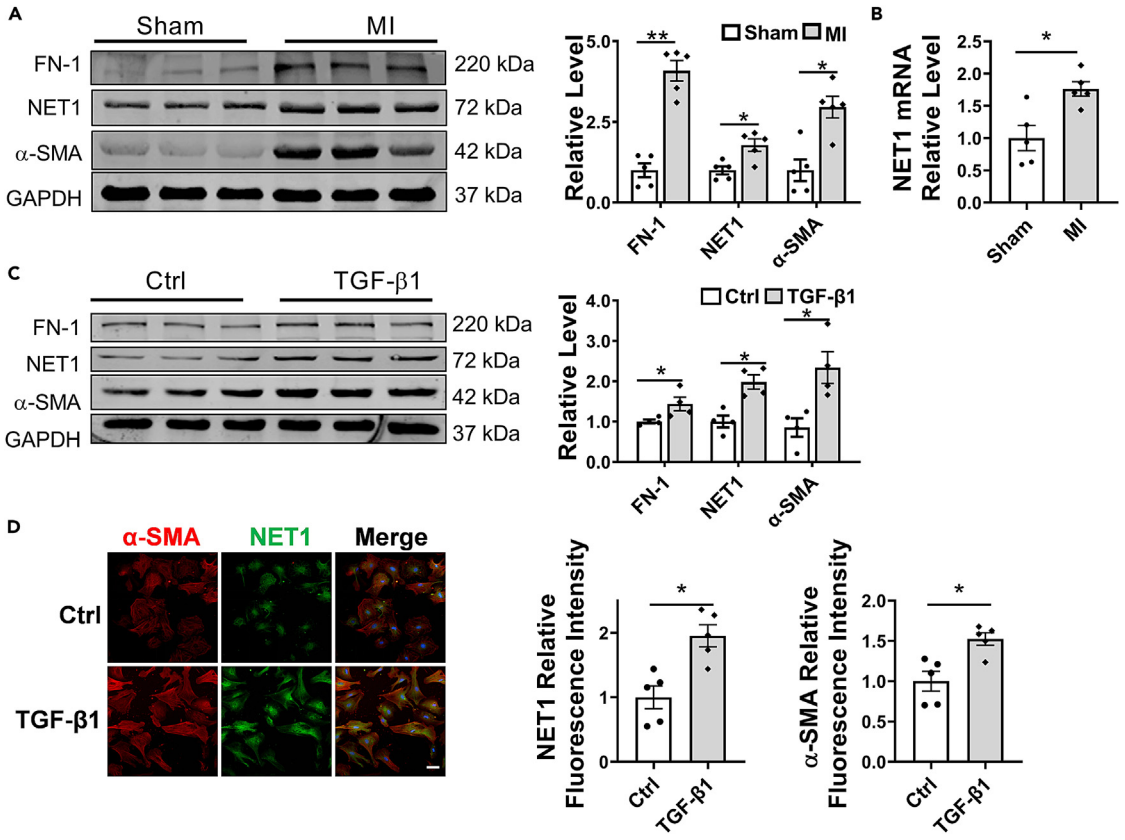

Figure 1. NET1 expression is increased in the cardiac fibrosis model

(A) Western blot was used to detect the changes of FN-1, α-SMA, and NET1 proteins, which were related to fibrosis in myocardial infarction tissue, and GAPDH was used as an internal reference. n = 5, **p = 0.0079, *p = 0.0476, *p = 0.0159 MI vs. Sham by Mann Whitney test.

(B) qRT-PCR was used to detect the changes of NET1 mRNA in cardiac fibrosis. n = 4, *p = 0.0159 MI vs. Sham by Mann Whitney test.

(C) Western blot was used to detect the changes of FN-1, α-SMA, and NET1 proteins in TGF-β1-treated group. n = 4, *p = 0.0286 TGF-β1 vs. Ctrl by Mann Whitney test.

(D) Representative image of cardiac fibroblasts stained with α-SMA antibody (Red) and NET1 antibody (Green). The levels of NET1 and α-SMA were measured by quantitative immunofluorescence. Scale bar: 50 μm, magnification 200×. n = 5, *p = 0.0159 TGF-β1 vs. Ctrl (Left panel), *p = 0.0159 TGF-β1 vs. Ctrl (Right panel) by Mann Whitney test. For all statistical plots, the data are presented as mean ± SEM.

However, although NET1 has been implicated in cardiac fibrosis, little is known about its involvement. Therefore, this study aimed to explore the mechanism by which NET1 regulates cardiac fibrosis.

RESULTS

NET1 expression was increased in the cardiac fibrosis model

To determine the expression of NET1 in cardiac fibrosis, we used an MI mouse model established by ligating the left anterior descending coronary artery to induce cardiac fibrosis. After 1 week, the expression of fibrotic marker proteins FN-1 and α-SMA, as well as that of NET1, was examined using western blot. The results showed significantly higher levels of FN-1, α-SMA, and NET1 in the MI group than in the sham group (Figure 1A). The mRNA expression of NET1 was also significantly higher on quantitative reverse transcription polymerase chain reaction (Figure 1B). These results support that the cardiac fibrosis model induced by MI was successful, and NET1 expression was increased in cardiac fibrosis tissue.

Transforming growth factor β1 (TGF-β1) (10 ng/mL) was used *in vitro* to induce fibrosis in cardiac fibroblasts. Expression levels of the fibrotic markers FN-1 and α-SMA were significantly increased in the TGF-β1-treated group. NET1 protein levels were significantly higher in the TGF-β1 group than in the control group (Figure 1C). For the level of NET1 and α-SMA measured by quantitative immunofluorescence, the fluorescence intensity of both NET1 and α-SMA was significantly enhanced by TGF-β1 treatment (Figure 1D). These results indicate that NET1 expression was increased in cardiac fibrosis induced by TGF-β1.

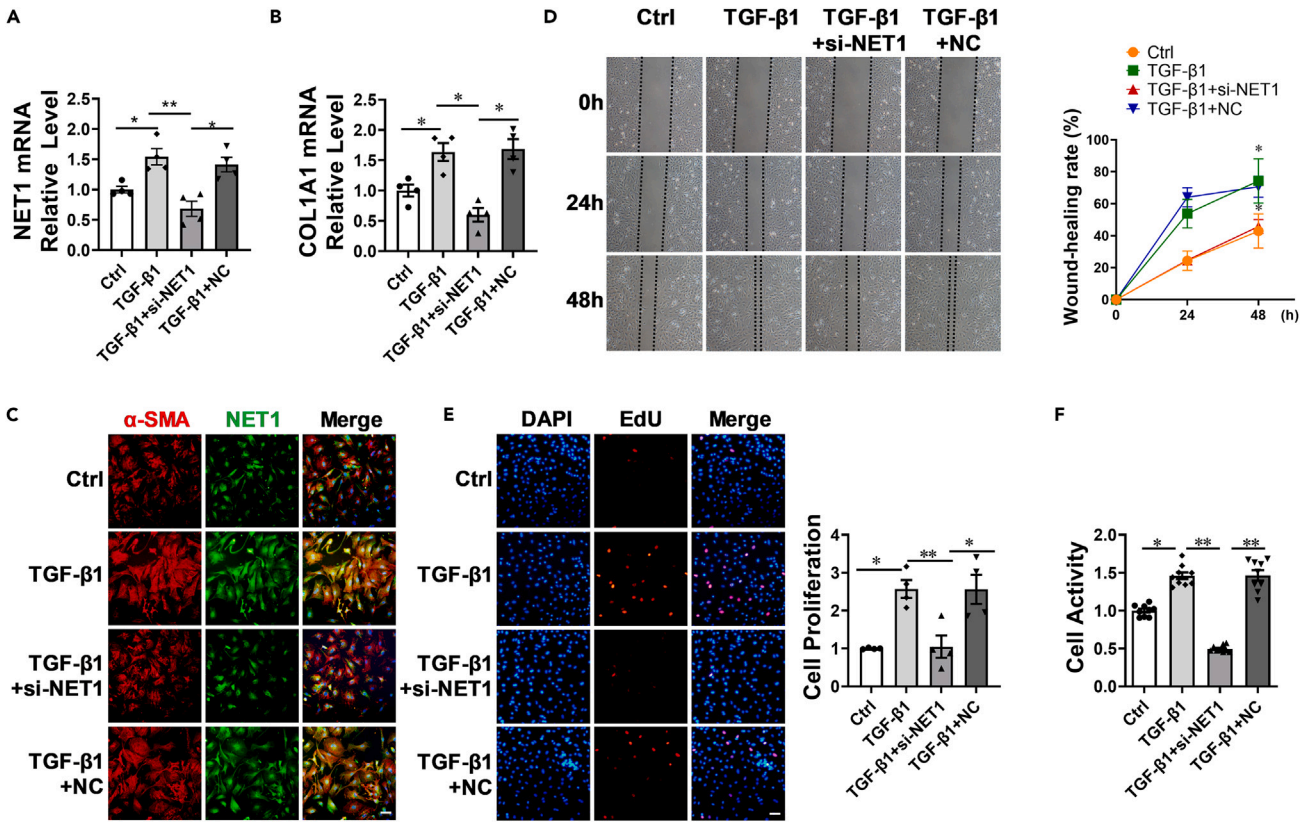

Figure 2. Effect of NET1 knockdown on TGF-β1-induced cardiac fibroblasts

(A) mRNA change of NET1, n = 4, *p = 0.0286 TGF-β1 vs. Ctrl by Mann Whitney test. **p = 0.0084 TGF-β1 + si-NET1 vs. TGF-β1 , *p = 0.0360 vs. TGF-β1 + si-NET1 vs. TGF-β1 + NC by Kruskal-Wallis test.

(B) mRNA of collagen I (COL1A1) was detected by qRT-PCR, n = 4, *p = 0.0286 TGF-β1 vs. Ctrl by Mann Whitney test. *p = 0.0360 TGF-β1 + si-NET1 vs. TGF-β1 , *p = 0.0140 TGF-β1 + si-NET1 vs. TGF-β1 + NC by Kruskal-Wallis test.

(C) Representative image of cardiac fibroblasts stained with α-SMA antibody (Red) and NET1 antibody (Green). Scale bar: 50 μm, magnification 200×.

(D) The migration of cardiac fibroblast was detected by scratch assay, n = 5, *p = 0.0452 TGF-β1 vs. Ctrl, *p = 0.0277 TGF-β1 + si-NET1 vs. TGF-β1, *p = 0.0452 TGF-β1 + si-NET1 vs. TGF-β1 + NC by Kruskal-Wallis test.

(E) The proliferative ability of cardiac fibroblasts was detected by EdU kit. Scale bar: 50 μm, magnification 200×, n = 4, *p = 0.0313 TGF-β1 vs. Ctrl, **p = 0.0075 TGF-β1 + si-NET1 vs. TGF-β1, *p = 0.0143 TGF-β1 + si-NET1 vs. TGF-β1 + NC by Kruskal-Wallis test.

(F) The viability of cardiac fibroblasts was detected by MTT assay, n = 9, *p = 0.0465 TGF-β1 vs. Ctrl, **p < 0.0001 TGF-β1 + si-NET1 vs. TGF-β1, **p < 0.0001 TGF-β1 + si-NET1 vs. TGF-β1 + NC by Kruskal-Wallis test. For all statistical plots, the data are presented as mean ± SEM.

Effect of NET1 knockdown on TGF-β1-induced cardiac fibroblasts

To evaluate the functional role of NET1 in TGF-β1-induced mouse primary cardiac fibroblasts, si-NET1 and its negative control (NC) were simultaneously transfected for 24 h. The results showed that mRNA expression levels of NET1 and collagen I were significantly increased in the TGF-β1-induced group. Compared to the TGF-β1 group, the TGF-β1 + si-NET1 group showed significantly lower mRNA levels of NET1 and fibrosis markers. NET1 knockdown inhibited the TGF-β1-induced increase in collagen I levels (Figures 2A and 2B). Immunofluorescence staining was also performed in cardiac fibroblasts, which indicated lower expression of NET1 and α-SMA in TGF-β1 + si-NET1 group (Figure 2C). The results showed that NET1 knockdown inhibits the transformation of fibroblasts into myofibroblasts.

A cell scratch assay to evaluate the level of fibroblast migration showed that TGF-β1 treatment promoted fibroblast migration. Meanwhile, NET1 knockdown reversed the increase in fibroblast migration induced by TGF-β1 (Figure 2D). In the TGF-β1 group, the number of EdU-positive cells was significantly increased, whereas the number of EdU-positive cells was significantly decreased after NET1 knockdown (Figure 2E). Fibroblast viability was significantly higher in the TGF-β1 group than in the control group, while it was significantly lower in the TGF-β1 + si-NET1 group than in the TGF-β1 + NC group or the TGF-β1 group (Figure 2F). These results suggest that NET1 knockdown inhibits TGF-β1-induced proliferation and migration of cardiac fibroblasts.

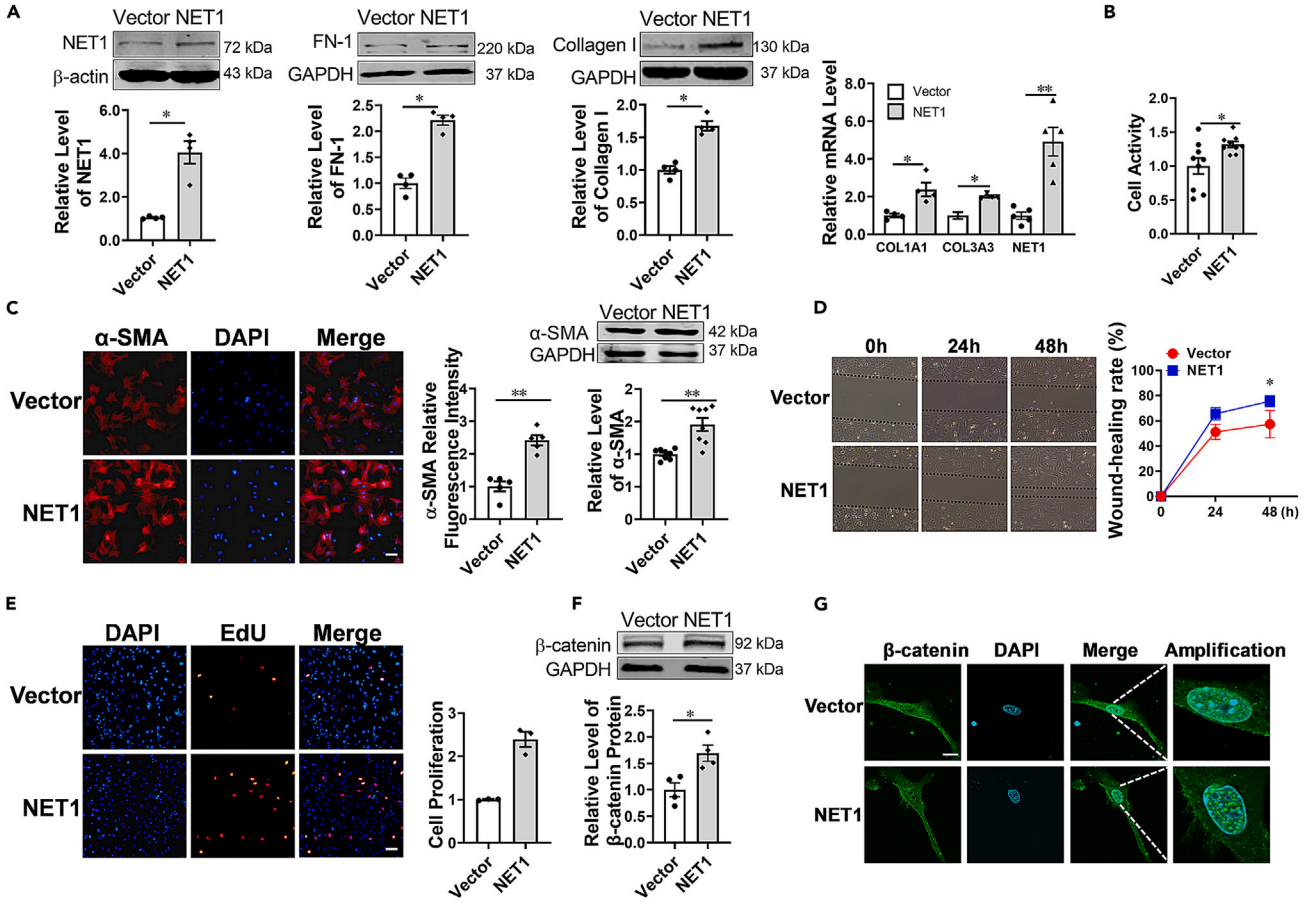

Figure 3. Effect of NET1 overexpression on cardiac fibroblasts

(A) Western blot was used to detect the protein expression levels of NET1, FN-1, and collagen I in cardiac fibroblasts transfected with NET1 overexpression plasmid, n = 4, *p = 0.0286 NET1 vs. Vector by Mann Whitney test. qRT-PCR was used to detect NET1, COL1A1 in fibroblasts and COL3A3 mRNA expression levels. n = 4–5, *p = 0.0286, *p = 0.0286, **p = 0.0079 NET1 vs. Vector by Mann Whitney test.

(B) Fibroblast viability was detected by MTT assay, n = 9, *p = 0.0244 NET1 vs. Vector by Mann Whitney test.

(C) The expression of myofibroblast marker α-SMA was detected by immunofluorescence (n = 5, **p = 0.0079) and western blot (n = 8, **p = 0.0019). NET1 vs. Vector by Mann Whitney test, Scale bar: 50 μm, magnification 200×.

(D) Fibroblast migration was detected by cell scratch assay. n = 4, *p = 0.0286 NET1 vs. Vector by Mann Whitney test.

(E) Fibroblast proliferation detected by Edu kit. Scale bar: 50 μm, magnification 200×, n = 3, p = 0.1000 NET1 vs. Vector by Mann Whitney test.

(F) Western blot was used to detect the protein level of β-catenin. n = 4, *p = 0.0286 NET1 vs. Vector by Mann Whitney test. For all statistical plots, the data are presented as mean ± SEM.

(G) Confocal microscopy was used to detect the expression of β-catenin in the nuclei of fibroblasts transfected with NET1 overexpression plasmid and Vector. Scale bar: 10 μm.

Effect of overexpression of NET1 on cardiac fibroblasts

We constructed a pcDNA3.1 vector carrying NET1 gene (GenBank: NM_001047159.2) for overexpression to investigate the effects of NET1 on cardiac fibrosis in mice. NET1-overexpressing plasmid in the vector was transfected into cardiac fibroblasts. Compared to the vector group, the NET1 group showed significantly higher protein and mRNA levels of NET1, and NET1 overexpression promoted the expression of FN-1 and collagen I in cardiac fibroblasts (Figure 3A). Fibroblast cell viability was significantly increased after transfection with NET1-overexpressing plasmid (Figure 3B). α-SMA expression detected by immunofluorescence and western blot was significantly higher in the NET1 group than in the vector group. NET1 overexpression enhanced cardiac fibroblast activation (Figure 3C). The ability of cells to migrate to the middle blank area was significantly higher in the NET1 group than in the control group, indicating that NET1 overexpression can significantly increase the proliferation and migration of cardiac fibroblasts (Figure 3D). The number of positive cells marked by EdU in the NET1 group was higher than that in the vector group, but the difference was not significant (Figure 3E).

β-Catenin can promote the transformation of fibroblasts to myofibroblasts and stimulate the pathological process of cardiac fibrosis.[7] Our results showed significantly higher expression levels of β-catenin in the NET1 group than in the vector group (Figure 3F). The nuclear

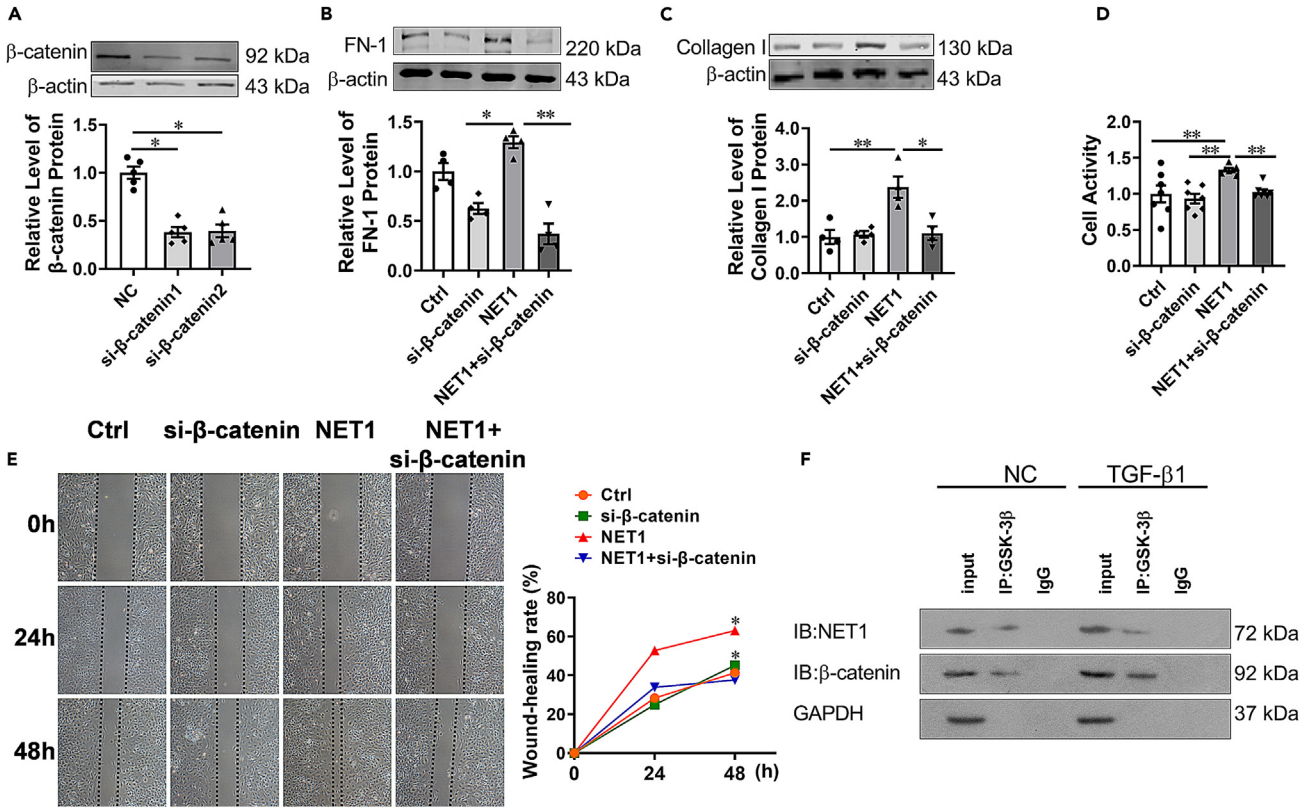

Figure 4. NET1 may be involved in cardiac fibrosis through β-catenin

(A) Cardiac fibroblasts were transfected with si-β-catenin and NC, and the protein level of β-catenin was detected by western blot. n = 5,*p = 0.0175 si-β-catenin1 vs. NC, *p = 0.0327 si-β-catenin2 vs. NC by Kruskal-Wallis test.

(B and C) Fibrosis marker protein FN-1 (n = 4, **p = 0.0011 NET1 + si-β-catenin vs. NET1 by Kruskal-Wallis test) and (C) collagen I expression was detected by western blot. n = 4, **p = 0.0075 NET1 vs. Ctrl, *p = 0.0259 NET1 + si-β-catenin vs. NET1 by Kruskal-Wallis test.

(D) MTT method was used for detection of fibroblast viability. n = 7, **p = 0.0093 Ctrl vs. NET1, **p = 0.0063 NET1 + si-β-catenin vs. NET1 by Kruskal-Wallis test.

(E) Fibroblast migration ability was detected by cell scratch method. n = 4, *p = 0.0166 Ctrl vs. NET1, **p = 0.0003 NET1 + si-β-catenin vs. NET1 by Kruskal-Wallis test. For all statistical plots, the data are presented as mean ± SEM.

(F) Co-immunoprecipitation (Co-IP) was performed to verify GSK3β protein interaction with NET1 and β-catenin.

expression of β-catenin in the nuclei of fibroblasts overexpressing NET1, as observed by confocal microscopy, was higher in the NET1 group (Figure 3G).

NET1 may be involved in cardiac fibrosis through β-catenin

We investigated whether knockdown β-catenin affected the fibrotic effect of NET1 in Figure 4. Compared to the NC group, the β-catenin knockdown group had significantly lower expression level of β-catenin in fibroblasts (Figure 4A). The protein levels of FN-1 and collagen I were significantly lower in the NET1 + si-β-catenin group than in the NET1 group (Figures 4B and 4C). Unlike in the control group, the si-β-catenin group displayed no significant effect on the viability of fibroblasts, and cell viability was more significantly inhibited in the NET1 + si-β-catenin group than in the NET1 group (Figure 4D). The scratch test revealed that in contrast to the control group, NET1 significantly promoted the migration of fibroblasts. Compared to the NET1 group, the NET1 + si-β-catenin group showed more significantly inhibited cell migration (Figure 4E). This suggests that β-catenin plays an important role in NET1-induced fibroblast-generating collagen, cell vitality, and cell migration. Thus, NET1 may affect the migration and viability of cardiac fibroblasts via β-catenin. Co-immunoprecipitation assays showed that NET1 and β-catenin could form a complex with glycogen synthase kinase 3 beta (GSK3β), indicating that both NET1 and β-catenin could bind GSK3β (Figure 4F).

To further confirm that NET1 overexpression is involved in cardiac fibrosis through β-catenin, we investigated the expression of β-catenin and its nuclear translocation in NET1 knockdown cells (Figure 5A). The results showed no significant difference in the expression of β-catenin and its nuclear translocation between NET1 knockdown cells and the negative control group. However, β-catenin expression in the nuclei of fibroblasts was lower in the TGF-β1 + si-NET1 group than in the TGF-β1 + NC group. Detection of NET1 overexpression on β-catenin showed

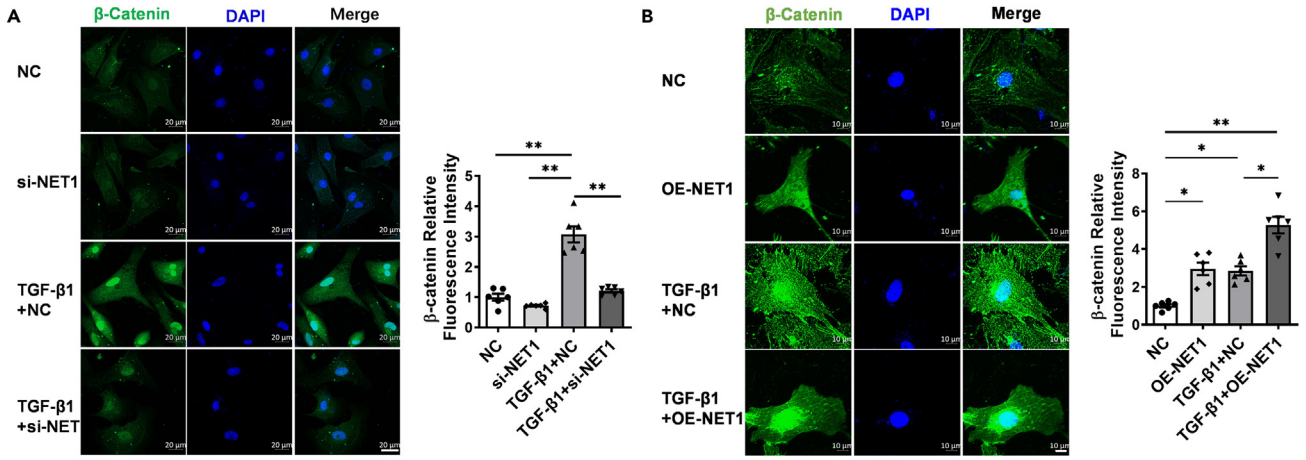

Figure 5. Effects of overexpression or knockdown of NET1 on β-catenin signaling pathways

(A) IF staining of β-catenin and quantitative analysis of β-catenin treated with or without si-NET1. n = 6, **p = 0.0037 TGF-β1 + NC vs. NC by Kruskal-Wallis test, **p = 0.0022 TGF-β1 + si-NET1 vs. TGF-β1 + NC by Mann Whitney test, Scale bar: 20 μm.

(B) IF staining of β-catenin and quantitative analysis of β-catenin treated with or without overexpression NET1. n = 6, *p = 0.0179 OE-NET1 vs. NC, *p = 0.0305 TGF-β1 + NC vs. NC, **p < 0.0001 TGF-β1 + OE-NET1 vs. NC, *p = 0.0338 TGF-β1 + OE-NET1 vs. TGF-β1 + NC, Scale bar: 10 μm. For all statistical plots, the data are presented as mean ± SEM.

higher β-catenin expression in the TGF-β1 + OE-NET1 group (overexpression-NET1, OE-NET1) than in the TGF-β1 + NC group (Figure 5B). These results demonstrate that NET1 promotes β-catenin expression in the nucleus.

Effects of GSK3β knockdown on TGF-β1-induced cardiac fibrosis

When Wnt signaling pathway is OFF, GSK3β forms a multimeric complex with APC, Axin, and β-catenin and phosphorylates the N terminus of β-catenin, leading to its degradation mediated by ubiquitin/proteasomes. To clarify whether GSK3β acted as a bridge between NET1 and β-catenin, we examined the role of GSK3β in TGF-β1-induced fibroblast activation. Western blot results showed that the level of NET1 was not significantly different between the TGF-β1 + siGSK3β group and the TGF-β1 group (Figure 6A). Meanwhile, the protein levels of collagen I and hydroxyproline (collagen content) were lower in the TGF-β1 + siGSK3β group than in the TGF-β1 group (Figure 6B). The fluorescence intensity of α-SMA in the TGF-β1 + siGSK3β group was also lower than that in the TGF-β1 group (Figure 6C). EdU cell proliferation assay showed that the number of EdU-labeled positive cells was significantly increased in the TGF-β1 and TGF-β1 + NC groups. Meanwhile, the number of EdU-positive cells was significantly lower in the TGF-β1 + siGSK3β group than in the TGF-β1+siNC group (Figure 6D).

The cell scratch assay showed that the ability of cells to migrate within the TGF-β1 + siGSK3β group was significantly weaker than in the TGF-β1 + siNC group (Figure 6E). Compared to the TGF-β1 + siNC group, the TGF-β1 + siGSK3β group showed lower protein level of GSK3β (Figure 6F). GSK3β knockdown significantly inhibited the proliferation and migration of cardiac fibroblasts under conditions induced by TGF-β1 (Figures 6D and 6E). The effect of GSK3β knockdown on the TGF-β1-induced GSK3β/β-catenin pathway in cardiac fibroblasts was detected by immunofluorescence (Figures 6G and 6H). The fluorescence intensity of GSK3β-S9 seems to be decreased in the TGF-β1 + siGSK3β group (Figure 6H). Immunofluorescence and western blot analysis showed that β-catenin entered the nucleus in the TGF-β1 and TGF-β1 + NC groups. Compared to the TGF-β1 group, the TGF-β1 + siGSK3β group had less β-catenin entering the nucleus (Figure 6I). These results showed GSK3β knockdown inhibited nuclear accumulation of β-catenin in fibroblasts induced by TGF-β1.

Effect of overexpression-NET1 on GSK3β/β-catenin and other signaling pathways

Compared to the NC group, knockdown of GSK3β in cardiac fibroblasts had no effect on the expression of NET1 and collagen (Figures 7A and 7B). The collagen content (hydroxyproline levels in Figure 7B right panel) and cell proliferation ratio (Figure 7D) in the NET1+ siGSK3β group were higher than those in the siGSK3β group. When siGSK3β was knocked down, NET1 can also promote collagen production and cell proliferation. This indicated that regulation of GSK3β/β-catenin signaling by NET1 may be non-specific. Immunofluorescence results showed that the fluorescence intensity of α-SMA in the NET1 + siGSK3β group was lower than that in the NET1 group (Figure 7C). The level of GSK3β was significantly decreased in NET1 + siGSK3β group, compared to NET1 compared to siGSK3β (Figure 7G). The number of EdU-labeled positive cells was no change in the NET1 + siGSK3β and siGSK3β groups (Figure 7E). Compared to the control group, the NET1 group showed higher levels of β-catenin protein expression; however, β-catenin levels were unaffected by GSK3β knockdown (Figure 7F). Immunofluorescence results showed that the fluorescence intensity of GSK3β-S389, GSK3β-S9, and β-catenin in the NET1 + siGSK3β group was lower than that in the NET1 group (Figures 7H and 7I). NET1 overexpression may play a role by affecting the phosphorylated form of GSK3β. The previously described results indicate that GSK3β knockdown is not a necessary condition for NET1 to promote β-catenin and regulate fibrosis.

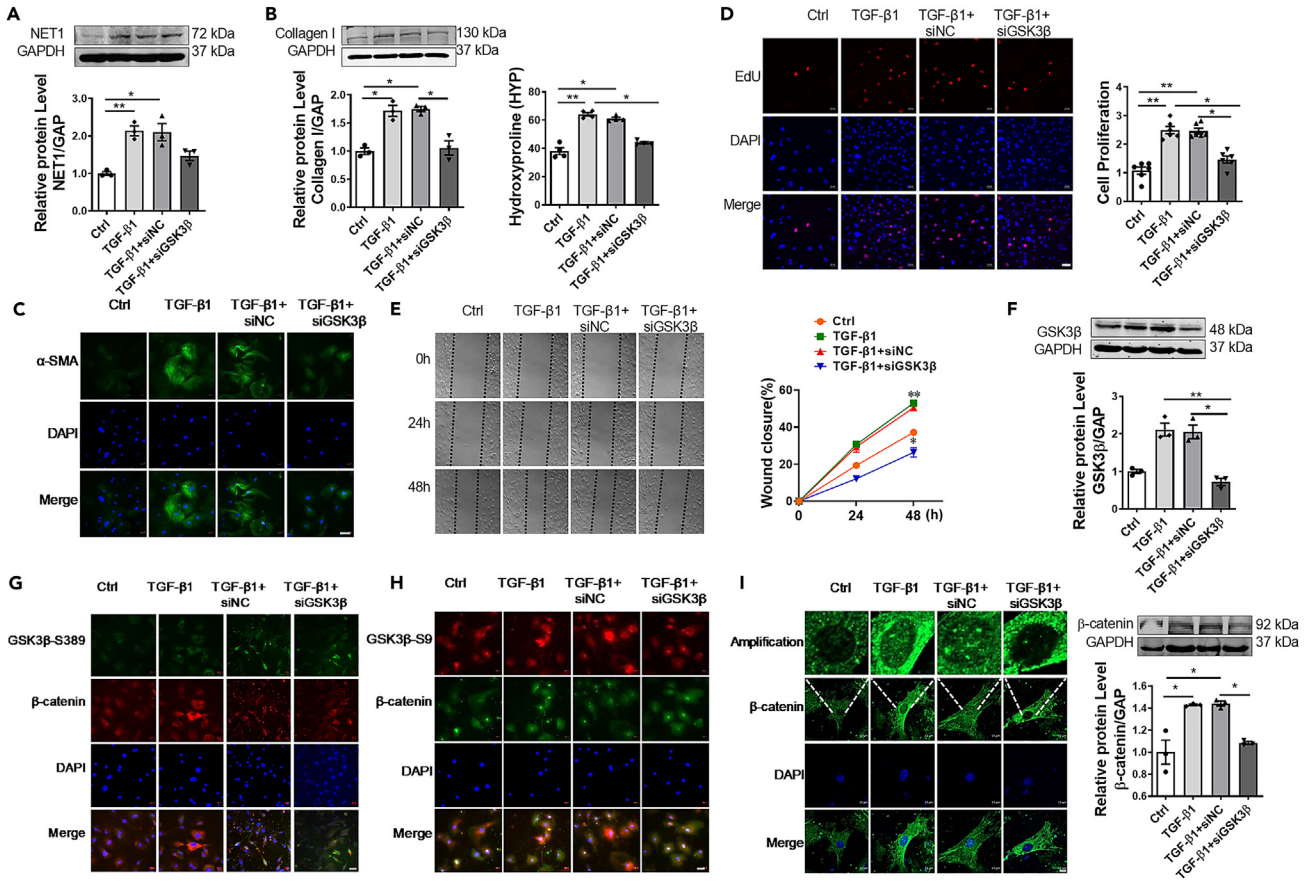

Figure 6. Effects of GSK3β knockdown on TGF-β1-induced cardiac fibrosis

(A and B) Expression level of NET1 (n = 3, **p = 0.0092 TGF-β1 vs. Ctrl, *p = 0.0127 TGF-β1 + siNC vs. Ctrl by Kruskal-Wallis test) (B) collagen I (n = 3, *p = 0.0415 TGF-β1 vs. Ctrl, *p = 0.0315 TGF-β1 + siNC vs. Ctrl, *p = 0.0415 TGF-β1 + siGSK3β vs. TGF-β1 + siNC) and hydroxyproline (n = 4, **p = 0.0014 TGF-β1 vs. Ctrl, *p = 0.0213 TGF-β1 + siNC vs. Ctrl, *p = 0.0143 TGF-β1 + siGSK3β vs. TGF-β1 by Kruskal-Wallis test.

(C) α-SMA after knockdown GSK3β in cardiac fibroblasts. Scale bar: 20 μm, magnification, 200×.

(D) EdU staining was used to detect fibroblast proliferation. Scale bar: 20 μm, magnification, 200×. n = 6, **p = 0.0005 TGF-β1 vs. Ctrl, **p = 0.0004 TGF-β1 + siNC vs. Ctrl, *p = 0.0160 TGF-β1 + siGSK3β vs. TGF-β1 + siNC by Kruskal-Wallis test.

(E) The migration of fibroblasts was detected by scratch experiment. n = 3, **p = 0.0046, TGF-β1 + siGSK3β vs. TGF-β1, *p = 0.0235, TGF-β1 + siGSK3β vs. TGF-β1 + siNC by Kruskal-Wallis test.

(F) Expression level of GSK3β after knockdown GSK3β in cardiac fibroblasts. n = 3, **p = 0.0055, TGF-β1 + siGSK3β vs. TGF-β1, *p = 0.0201, TGF-β1 + siGSK3β vs. TGF-β1 + siNC by Kruskal-Wallis test.

(G and H) Expression level of GSK3β-S389, and (H) GSK3β-S9 after knockdown GSK3β in cardiac fibroblasts. Scale bar: 20 μm, magnification, 200×.

(I) Confocal microscopy was used to detect the expression of β-catenin in the nuclei of fibroblasts transfected with TGF-β1 and knockdown GSK3β. Expression level of β-catenin after knockdown GSK3β in cardiac fibroblasts. n = 3, *p = 0.0415 TGF-β1 vs. Ctrl, *p = 0.0174 TGF-β1 + siNC vs. Ctrl, *p = 0.0415 TGF-β1 + siGSK3β vs. TGF-β1 + siNC by Kruskal-Wallis test. For all statistical plots, the data are presented as mean ± SEM.

To determine whether NET1 affects other signaling pathways (such as TGF-β1) involved in cardiac fibrosis, correlation analysis was performed to determine the relationship between NET1 and the signaling pathways of cardiac fibrosis. The results showed no significant correlation between signaling pathways and NET1 in GSE220612, GSE211380, GSE206281, GSE153485, and GSE147365. However, NET1 was positively correlated with the Notch signaling pathway in GSE183272 and GSE181872. Furthermore, NET1 was positively correlated with TGF-β1 signaling and MAPK pathways in GSE181872 (Figures S1 and S2). NET1 (transfected with si-NET1) expression was knocked down in fibroblasts, and the level of *p*-Smad3 in the TGF-β1 signaling pathway in fibroblasts was detected (Figure S3). Immunofluorescence results showed that NET1 knockdown alone did not affect the expression of *p*-Smad3, but under TGF-β1-induced conditions, NET1 knockdown reduced the amount of *p*-Smad3 entering the nucleus. Western blot also showed that NET1 knockdown reduced the expression of *p*-Smad3 (Figure S3C). After transfecting the NET1-overexpressing plasmid into fibroblasts, *p*-Smad3 expression in fibroblasts was detected. The immunofluorescence results showed that compared with the NC, overexpression of NET1 promoted the entry of *p*-Smad3 into the nucleus in OE-NET1 (Figure S3B).

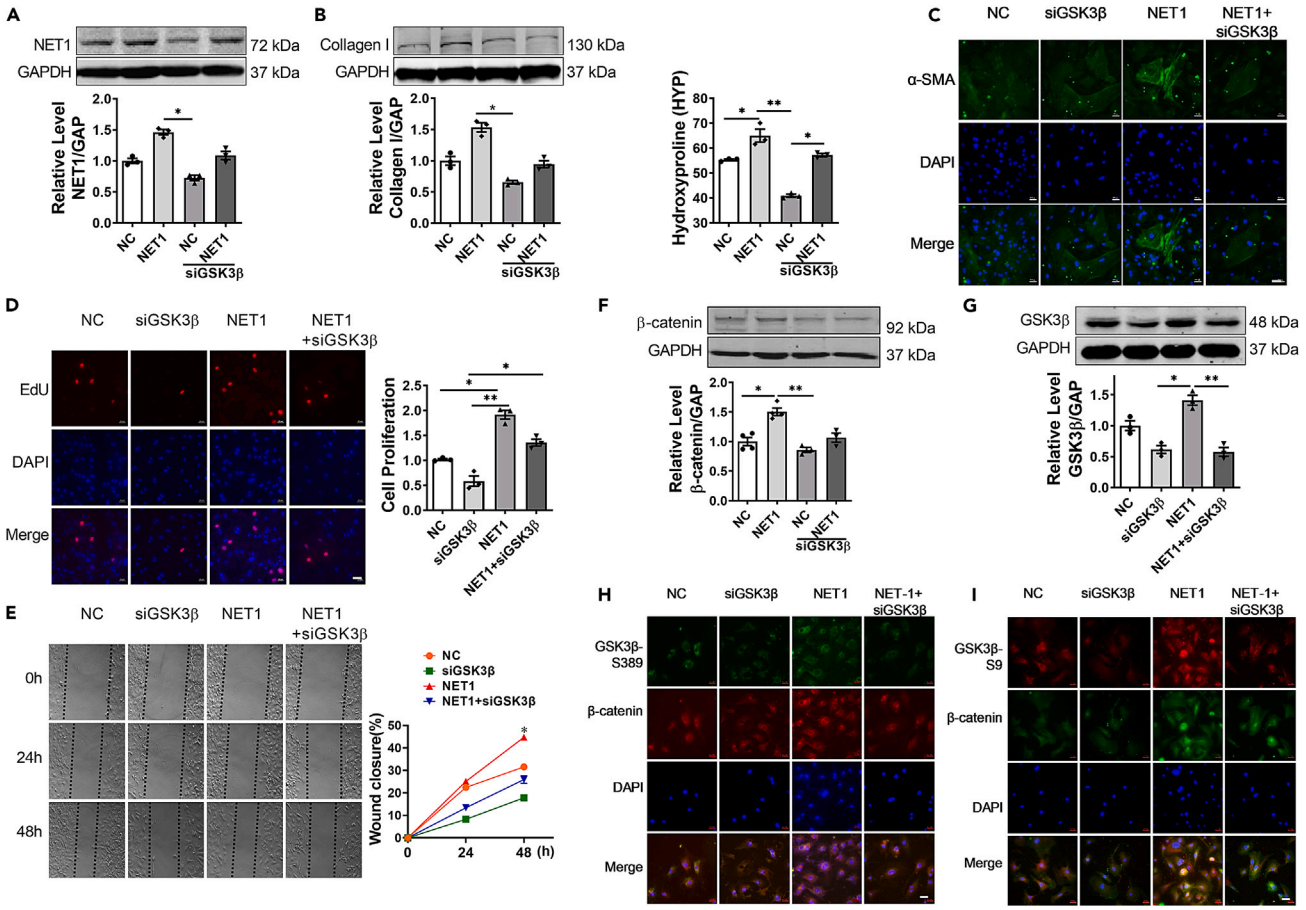

Figure 7. Effects of GSK3β knockdown on cardiac fibrosis induced by NET1 overexpression

(A) Expression level of NET1 after overexpression NET1 and knockdown GSK3β in cardiac fibroblasts. n = 3, **p = 0.0022 NET1 vs. NC + siGSK3β, n = 3, by Kruskal-Wallis test.

(B) Expression level of collagen I (n = 3, **p = 0.0022 NET1 vs. NC + siGSK3β) and hydroxyproline (n = 3, *p = 0.0415 NC vs. NET1, **p = 0.0022 NET1 vs. NC + siGSK3β, *p = 0.0415 NET1+ siGSK3β vs. NC + siGSK3β) after overexpression NET1 and knockdown GSK3β in cardiac fibroblasts.

(C) Expression level of α-SMA after overexpression NET1 and knockdown GSK3β in cardiac fibroblasts. Scale bar: 20 μm, magnification, 200×.

(D) EdU staining was used to detect fibroblast proliferation, Scale bar: 20 μm, magnification, 200×. n = 3. *p = 0.0415 NC vs. NET1, **p = 0.0022 siGSK3β vs. NET1, *p = 0.0415 NET1 + siGSK3β vs. siGSK3β by Kruskal-Wallis test.

(E) The migration of fibroblasts was detected by scratch experiment. n = 3, *p = 0.0134 siGSK3β vs. NET1 by Kruskal-Wallis test.

(F) Expression level of β-catenin after overexpression NET1 and knockdown GSK3β in cardiac fibroblasts. n = 3, *p = 0.0280 NC vs. NET1, **p = 0.0029 NET1 vs. NC + siGSK3β, by Kruskal-Wallis test.

(G) Expression level of GSK3β after overexpression NET1 and knockdown GSK3β in cardiac fibroblasts. n = 3, *p = 0.0174 siGSK3β vs. NET1, **p = 0.0066 NET1 + siGSK3β vs. NET1 by Kruskal-Wallis test. For all statistical plots, the data are presented as mean ± SEM.

(H and I) Expression level of GSK3β-S389 (Green), GSK3β-S9 (Red) (I), and β-catenin after overexpression NET1 and knockdown GSK3β in cardiac fibroblasts. Scale bar: 20 μm, magnification, 200×.

Effects of NET1 in myocardial infarction in mice

The protein expression levels of α-SMA, collagen, and NET1 were significantly higher in the MI group than those in the sham group (Figures 8A–8C). The protein expression levels of α-SMA, collagen, and NET1 were significantly lower in the knockout (KO) + MI group than in the MI group. NET1 knockdown reduced cardiac fibrosis in MI mice. Figure 8D shows that the β-catenin protein expression level in the MI group was 2.27 ± 0.16 times higher than that in the sham group, and the β-catenin protein expression level in the KO + MI group was lower than that in the MI group. These results supported that NET1 knockout reduced the protein expression of β-catenin in the heart tissue of mice with myocardial infarction. The expressions of GSK3β-S389 and GSK3β-S9 in the KO group were decreased in contrast to the MI group (Figure 8E). In the control + MI group, the nuclei were pyknotic, the mitochondria were swollen, and the myofilaments were broken and disordered. In the KO group, the nuclei were normal, the mitochondria were arranged regularly along the myofilaments, and the sarcomeres and mitochondria were not swollen. In the KO-MI group, the condition was relieved and most of the mitochondrial structure was normal, some

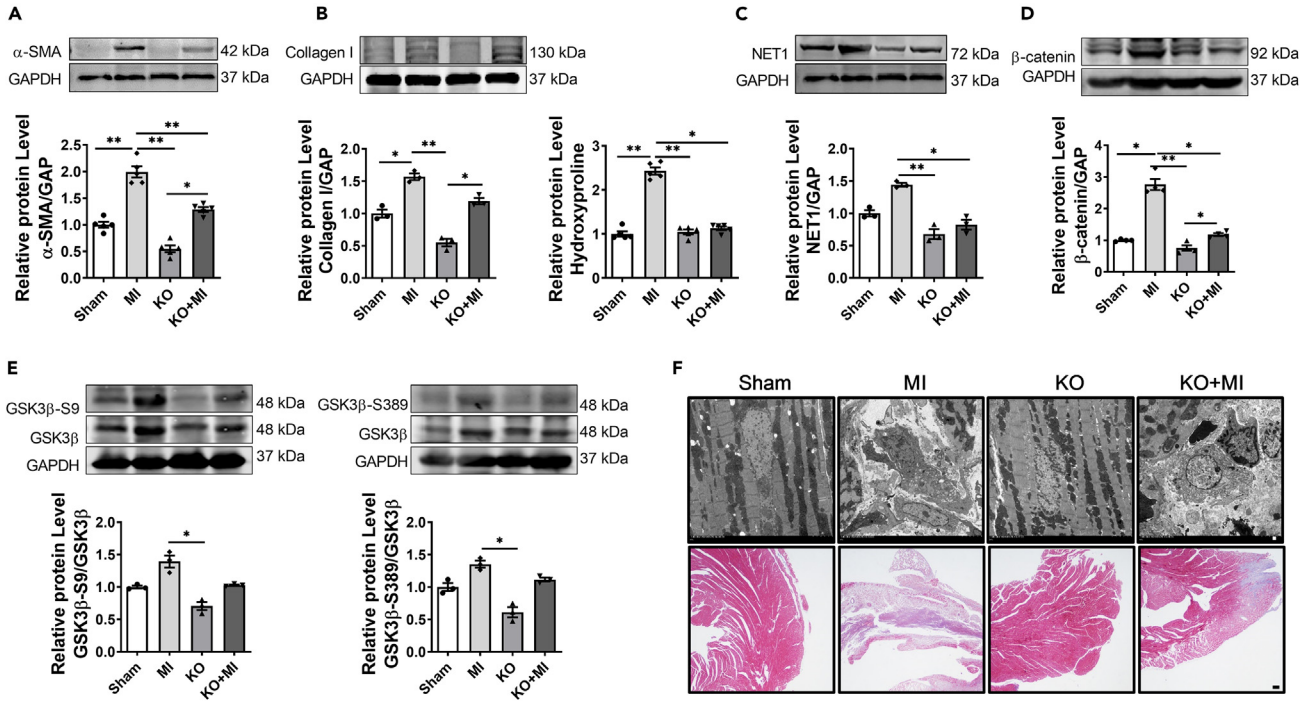

Figure 8. The role of NET1 in myocardial infarction in mice

(A) The protein level of α-SMA in mouse model. n = 5, **p = 0.0088 Sham vs. MI, **p < 0.0001 MI vs. KO, **p = 0.0088 KO vs. KO + MI, by Kruskal-Wallis test, **p = 0.0079 KO + MI vs. MI by Mann Whitney test.

(B) The protein level of collagen I (n = 3, *p = 0.0415 Sham vs. MI, **p = 0.0022 MI vs. KO, *p = 0.0415 KO vs. KO + MI) and hydroxyproline in mouse model (n = 6, **p = 0.0013 Sham vs. MI, **p = 0.0046 MI vs. KO, *p = 0.0479 MI vs. KO + MI by Kruskal-Wallis test).

(C and D) The protein level of NET1 in mouse model. n = 3, **p = 0.0032 MI vs. KO, *p = 0.0415 MI vs. KO + MI. (D) The protein level of β-catenin in mouse MI model. n = 4, *p = 0.0143 Sham vs. MI, **p = 0.0005 MI vs. KO, *p = 0.0213 KO vs. KO + MI by Kruskal-Wallis test. *p = 0.0286 KO + MI vs. MI by Mann Whitney test.

(E) The protein level of GSK3β-S389 in mouse MI model. n = 3, *p = 0.0022 MI vs. KO by Kruskal-Wallis test. The protein level of GSK3β-S9 in mouse MI model. n = 3*p = 0.0022 MI vs. KO by Kruskal-Wallis test. For all statistical plots, the data are presented as mean ± SEM.

(F) Changes of myocardial ultrastructure in each group. The ultrastructure of cardiomyocytes was observed under electron microscope. Magnification, ×15000. Scale bar calibration: 2 μm; The heart tissues of mice in each group were observed by Masson staining. Masson staining was used to observe the heart tissue. Scale bar calibration: 100 μm.

ridges were loose, and the swelling was mild. Myocardial ultrastructural injury was mild. In Masson staining, the blue area of heart tissue in the KO + MI group was less than that in the control + MI group in the same area, and the ischemic tissue injury was less severe (Figure 8F).

DISCUSSION

In this study, the expression level of NET1 was significantly increased in the myocardial fibrosis mouse model and in the myocardial fibrosis model induced by TGF-β1. NET1-induced fibrosis was confirmed to be activated via promoting β-catenin nuclear translocation. This study revealed the role and mechanism of action of NET1 in myocardial fibrosis.

As a GEF family member, NET1 has GEF activity that promotes the dissociation of GDP from the Rho protein, thus enabling GTP to play a role.[8,9] As a member of the Rho guanine exchange factor family, NET1 activates Rho proteins by catalyzing the conversion of guanosine diphosphate to guanosine triphosphate and regulates cytoskeleton formation, gene transcription, vesicle trafficking, cell adhesion, migration, proliferation, and differentiation.[10–12] Current research on NET1 mainly focuses on its role in tumorigenesis.[13] Rho guanine exchange factors are involved in mediating the fiber response of cardiomyocytes and cardiac fibroblasts in response to physicochemical stimuli.[14] Notably, GEFs/RhoA is important as a pro-fibrotic signaling pathway in idiopathic pulmonary fibrosis.[15] NET1 and Rho signals are significantly enhanced during the EMT of SC-4 epithelial cells.[16] NET1 promotes the proliferation and migration of mouse embryonic fibroblasts.[17] In addition, NET1 can phosphorylate β-catenin through PAK-1 kinase, induce the transcription of downstream β-catenin signaling molecules, and promote embryonic development in zebrafish.[6] These studies suggest that NET1 may be involved in the process of myocardial fibrosis; however, it is yet to be confirmed.

The Wnt/β-catenin signaling pathway is a highly conserved signaling pathway in the evolution of species and is widely involved in embryonic development, organ formation, tissue regeneration, and other physiological processes.[18] The Wnt signaling pathway is closely related to myocardial fibrosis.[19–21] The GSK3β/β-catenin pathway plays an important role in the development of myocardial fibrosis. Overexpression of

β-catenin can promote the transformation of fibroblasts into myofibroblasts and promote secretion of extracellular matrix proteins.[22] Therefore, GSK3β has been established as an important upstream effector of β-catenin activity.

The current study found that NET1 expression increased during cardiac fibrosis both *in vivo* and *in vitro*. The results showed that NET1 is involved in regulating cardiac fibrosis by β-catenin. Unlike most protein kinases, GSK3β is normally active in unstimulated cells and is inhibited in response to various inputs. In the absence of NET1 overexpression, or closure of the Wnt/β-catenin pathway, GSK3β can target β-catenin for ubiquitination and proteasomal degradation. Based on the experimental results, we conclude that GSK3β, as a phosphatase, plays as a bridge connecting NET1 and β-catenin to form a complex, when NET1 expression is increased. The formation of the NET1-GSK3β-β-catenin complex reduces the degradation of β-catenin by ubiquitination and promotes the entry of β-catenin into the nucleus. In the GSK3β knockdown group, the bridge function of GSK3β was lost, and even with NET1 overexpression, the three complexes could not be formed, which promoted the degradation of β-catenin by ubiquitination. NET1 overexpression promoted the phosphorylation of GSK3β at Ser-9/Ser-389. This resulted in increased β-catenin activity and promoted β-catenin expression in the nucleus and significantly increased the proliferation and migration of cardiac fibroblasts. The mechanism may be that NET1 overexpression promotes the expression of β-catenin in the nuclei of fibroblasts by regulating the phosphorylation of GSK3β (Ser9 and Ser389). Overexpressed NET1 also activates TGF-β signaling and facilitates *p*-Smad3 entry into the nucleus. NET1 was involved in the crosstalk between GSK3β and the classical TGF-β-Smad3 cascade. This results in increased β-catenin activity, reduced degradation of β-catenin, and increased nuclear entry of β-catenin, which increase α-SMA, type I collagen, and fibronectin, thus promoting cardiac fibrosis.

GSK3β is a ubiquitously expressed and highly conserved serine/threonine kinase involved in regulating multiple cellular functions such as embryonic development, energy metabolism, cell motility, apoptosis, cell differentiation, and proliferation.[23] GSK3β is an essential component of the Wnt/Frizzled signaling pathway and regulates the balance between cytoplasmic accumulation and nuclear translocation of β-catenin. Numerous studies have demonstrated that GSK3β targets β-catenin for ubiquitination and proteasomal degradation. GSK3β, a key regulator of neuronal apoptosis, is one of the few protein kinases that can be inactivated via phosphorylation and inhibited by phosphorylation at Ser-9/Ser-389.[24] When Ser9 at the N terminus of GSK3β is phosphorylated, apparent inhibition of activity results in β-catenin accumulation and nuclear translocation.[25] Phosphorylation of GSK3β at S9 increases cell viability, attenuates apoptosis in H/R-injured H9C2 cardiomyocytes, and modulates hypertrophic cardiomyocyte growth and viability.[26–28] Given that GSK3β is an essential component of this degradation complex, its deletion leads to β-catenin accumulation and nuclear translocation, which leads to the activation of β-catenin-dependent gene programs.[29–33] Switching between phosphorylated and dephosphorylated states of GSK3β is a highly dynamic event that can affect various molecular pathways. As GSK3β-mediated phosphorylation of substrates often results in their inhibition, the end result of stimulus-induced inhibition of GSK3β is often the activation of its downstream targets.[34]

The bioinformatics and complementary experimental results support that NET1 may be related to other signaling pathways, rather than specifically acting on the Wnt/β-catenin signaling pathway. The GSK3β, β-catenin, and TGF-β1-Smad3 signaling networks function as a critical regulator of myocardial fibrosis in the diseased heart.[19] Crosstalk between GSK3β and the classical TGF-β1-Smad3 cascade is critical for the regulation of myocardial fibrosis in diseased hearts.[19] GSK3β exerts a critical brake on the classical TGF-β1-Smad3 pathway through direct interactions and also through β-catenin signaling. Our results support that the effect of NET1 on cardiac fibrosis may be the result of multiple targets and pathways, such as the Wnt signaling and the TGF-β signaling pathways. NET1 promotes cardiac fibrosis in mouse, and the effect of NET1 on cardiac fibrosis may be achieved by promoting β-catenin expression and nuclear translocation. Given the regulatory role of NET1 in myocardial fibrosis, further clarification of the role of NET1 in myocardial fibrosis may help to design new, more targeted treatments.

Limitations of the study

There are some limitations in this study. One limitation is that co-immunoprecipitation experiments confirm that NET1 can form a complex with GSK3β and β-catenin, suggesting that NET1 promotes nuclear translocation and accumulation of β-catenin. However, the specific binding sites of NET1, GSK3β, and β-catenin need further exploration. The other one is that NET1 can not only participate in cardiac fibrosis through Wnt/β-catenin but also affect the TGF-β/Smad3 pathway. However, the current research results do not fully explain the effect of NET1 on crosstalk of Wnt and TGF-β/Smad3 signaling. The future research will investigate the specific mechanism of NET1 targeting β-catenin, to explain the role of NET1 in the crosstalk between the TGF-β/Smad3 signaling pathways.

STAR★METHODS

Detailed methods are provided in the online version of this paper and include the following:

- KEY RESOURCES TABLE
- RESOURCE AVAILABILITY
  - Lead contact
  - Materials availability
  - Data and code availability
- EXPERIMENTAL MODEL AND STUDY PARTICIPANT DETAILS
  - Study approval
  - Mouse model of myocardial infarction
  - Cardiac fibroblast isolation and culture

SUPPLEMENTAL INFORMATION

Supplemental information can be found online at https://doi.org/10.1016/j.isci.2023.107888.

ACKNOWLEDGMENTS

Thanks to the National Natural Science Foundation of China for the funding and to each of the authors for their hard work. This study was supported by the National Natural Science Foundation of China (81870211, 82170299, 82003757, 81800362).

AUTHOR CONTRIBUTIONS

T.L., X.L., L.L., H.L., and H.S. designed the experiments. Y.W., Y. Li, Y. Liu, M.Z., C.L., and S.C. performed the cell experiments. X.X., X.L., W.C., and T.Y. contributed to the discussion of manuscript. Y.W., Y. Li, and M.Z. contributed to the animal experiments. T.L., X.X., H.Z., X.W., and Y.-H.Z. analyzed the data. X.X., X.L., and H.S. wrote the paper.

DECLARATION OF INTERESTS

The authors declare no competing interests.

INCLUSION AND DIVERSITY

We support inclusive, diverse, and equitable conduct of research.

Received: January 18, 2023
Revised: July 15, 2023
Accepted: September 7, 2023
Published: September 9, 2023

REFERENCES

1. Centurión, O.A., Alderete, J.F., Torales, J.M., García, L.B., Scavenius, K.E., and Miño, L.M. (2019). Myocardial Fibrosis as a Pathway of Prediction of Ventricular Arrhythmias and Sudden Cardiac Death in Patients With Nonischemic Dilated Cardiomyopathy. Crit. Pathw. Cardiol. *18*, 89–97. https://doi.org/10.1097/HPC.0000000000000171.
2. Holmström, L., Haukilahti, A., Vähätalo, J., Kenttä, T., Appel, H., Kiviniemi, A., Pakanen, L., Huikuri, H.V., Myerburg, R.J., and Junttila, J. (2020). Electrocardiographic associations with myocardial fibrosis among sudden cardiac death victims. Heart *106*, 1001–1006. https://doi.org/10.1136/heartjnl-2019-316105.
3. Kristelly, R., Gao, G., and Tesmer, J.J.G. (2004). Structural determinants of RhoA binding and nucleotide exchange in leukemia-associated Rho guanine-nucleotide exchange factor. J. Biol. Chem. *279*, 47352–47362. https://doi.org/10.1074/jbc.M406056200.
4. Carr, H.S., Cai, C., Keinänen, K., and Frost, J.A. (2009). Interaction of the RhoA exchange factor Net1 with discs large homolog 1 protects it from proteasome-mediated degradation and potentiates Net1 activity. J. Biol. Chem. *284*, 24269–24280. https://doi.org/10.1074/jbc.M109.029439.
5. Chan, A.M., Takai, S., Yamada, K., and Miki, T. (1996). Isolation of a novel oncogene, NET1, from neuroepithelioma cells by expression cDNA cloning. Oncogene *12*, 1259–1266.
6. Wei, S., Dai, M., Liu, Z., Ma, Y., Shang, H., Cao, Y., and Wang, Q. (2017). The guanine nucleotide exchange factor Net1 facilitates the specification of dorsal cell fates in zebrafish embryos by promoting maternal beta-catenin activation. Cell Res. *27*, 202–225. https://doi.org/10.1038/cr.2016.141.
7. Tao, H., Yang, J.J., Shi, K.H., and Li, J. (2016). Wnt signaling pathway in cardiac fibrosis: New insights and directions. Metabolism *65*, 30–40. https://doi.org/10.1016/j.metabol.2015.10.013.
8. Laurin, M., and Côté, J.F. (2014). Insights into the biological functions of Dock family guanine nucleotide exchange factors. Genes Dev. *28*, 533–547. https://doi.org/10.1101/gad.236349.113.
9. Rossman, K.L., Der, C.J., and Sondek, J. (2005). GEF means go: turning on RHO GTPases with guanine nucleotide-exchange factors. Nat. Rev. Mol. Cell Biol. *6*, 167–180. https://doi.org/10.1038/nrm1587.
10. Qin, H., Carr, H.S., Wu, X., Muallem, D., Tran, N.H., and Frost, J.A. (2005). Characterization of the biochemical and transforming

properties of the neuroepithelial transforming protein 1. J. Biol. Chem. *280*, 7603–7613. https://doi.org/10.1074/jbc.M412141200.

11. Anders, N., and Jürgens, G. (2008). Large ARF guanine nucleotide exchange factors in membrane trafficking. Cell. Mol. Life Sci. *65*, 3433–3445. https://doi.org/10.1007/s00018-008-8227-7.
12. Ulu, A., Oh, W., Zuo, Y., and Frost, J.A. (2018). Stress-activated MAPKs and CRM1 regulate the subcellular localization of Net1A to control cell motility and invasion. J. Cell Sci. *131*, jcs204644. https://doi.org/10.1242/jcs.204644.
13. Yang, X., Li, Y., Zhang, Y., and Liu, J. (2022). Circ_0000745 promotes acute lymphoblastic leukemia progression through mediating miR-494-3p/NET1 axis. Hematology *27*, 11–22. https://doi.org/10.1080/16078454.2021.2008590.
14. Numaga-Tomita, T., Kitajima, N., Kuroda, T., Nishimura, A., Miyano, K., Yasuda, S., Kuwahara, K., Sato, Y., Ide, T., Birnbaumer, L., et al. (2016). TRPC3-GEF-H1 axis mediates pressure overload-induced cardiac fibrosis. Sci. Rep. *6*, 39383. https://doi.org/10.1038/srep39383.
15. Lu, D., Aroonsakool, N., Yokoyama, U., Patel, H.H., and Insel, P.A. (2013). Increase in cellular cyclic AMP concentrations reverses the profibrogenic phenotype of cardiac myofibroblasts: a novel therapeutic approach for cardiac fibrosis. Mol. Pharmacol. *84*, 787–793. https://doi.org/10.1124/mol.113.087742.
16. Kawata, H., Shimada, N., Kamiakito, T., Komatsu, K., Morita, T., Ota, T., Obayashi, M., Shitara, K., and Tanaka, A. (2012). RhoC and guanine nucleotide exchange factor Net1 in androgen-unresponsive mouse mammary carcinoma SC-4 cells and human prostate cancer after short-term endocrine therapy. Prostate *72*, 1071–1079. https://doi.org/10.1002/pros.21511.
17. Chan, A.M., Takai, S., Yamada, K., and Miki, T. (1996). Isolation of a novel oncogene, NET1, from neuroepithelioma cells by expression cDNA cloning. Oncogene *12*, 1259–1266. undefined.
18. Sebio, A., Kahn, M., and Lenz, H.J. (2014). The potential of targeting Wnt/beta-catenin in colon cancer. Expert Opin. Ther. Targets *18*, 611–615. https://doi.org/10.1517/14728222.2014.906580.
19. Li, X., Wang, G., QiLi, M., Liang, H., Li, T., E, X., Feng, Y., Zhang, Y., Liu, X., Qian, M., et al. (2018). Aspirin Reduces Cardiac Interstitial Fibrosis by Inhibiting Erk1/2-Serpine2 and P-Akt Signalling Pathways. Cell. Physiol. Biochem. *45*, 1955–1965. https://doi.org/10.1159/000487972.
20. Gitau, S.C., Li, X., Zhao, D., Guo, Z., Liang, H., Qian, M., Lv, L., Li, T., Xu, B., Wang, Z., et al. (2015). Acetyl salicylic acid attenuates cardiac hypertrophy through Wnt signaling. Front. Med. *9*, 444–456. https://doi.org/10.1007/s11684-015-0421-z.
21. Akhmetshina, A., Palumbo, K., Dees, C., Bergmann, C., Venalis, P., Zerr, P., Horn, A., Kireva, T., Beyer, C., Zwerina, J., et al. (2012). Activation of canonical Wnt signalling is required for TGF-beta-mediated fibrosis. Nat. Commun. *3*, 735. https://doi.org/10.1038/ncomms1734.
22. Hahn, J.Y., Cho, H.J., Bae, J.W., Yuk, H.S., Kim, K.I., Park, K.W., Koo, B.K., Chae, I.H., Shin, C.S., Oh, B.H., et al. (2006). Beta-catenin overexpression reduces myocardial infarct size through differential effects on cardiomyocytes and cardiac fibroblasts. J. Biol. Chem. *281*, 30979–30989. https://doi.org/10.1074/jbc.M603916200.
23. Sharma, A.K., Thanikachalam, P.V., and Bhatia, S. (2020). The signaling interplay of GSK-3beta in myocardial disorders. Drug Discov. Today *25*, 633–641. https://doi.org/10.1016/j.drudis.2020.01.017.
24. Ma, S., Liu, S., Huang, Q., Xie, B., Lai, B., Wang, C., Song, B., and Li, M. (2012). Site-specific phosphorylation protects glycogen synthase kinase-3beta from calpain-mediated truncation of its N and C termini. J. Biol. Chem. *287*, 22521–22532. https://doi.org/10.1074/jbc.M111.321349.
25. Molagoda, I.M.N., Kang, C.H., Lee, M.H., Choi, Y.H., Lee, C.M., Lee, S., and Kim, G.Y. (2021). Fisetin promotes osteoblast differentiation and osteogenesis through GSK-3beta phosphorylation at Ser9 and consequent beta-catenin activation, inhibiting osteoporosis. Biochem. Pharmacol. *192*, 114676. https://doi.org/10.1016/j.bcp.2021.114676.
26. Takahashi-Yanaga, F. (2018). Roles of Glycogen Synthase Kinase-3 (GSK-3) in Cardiac Development and Heart Disease. J. UOEH *40*, 147–156.
27. Lal, H., Ahmad, F., Woodgett, J., and Force, T. (2015). The GSK-3 family as therapeutic target for myocardial diseases. Circ. Res. *116*, 138–149. https://doi.org/10.1161/CIRCRESAHA.116.303613.
28. Chen, M., Liu, Q., Chen, L., Zhang, L., Cheng, X., and Gu, E. (2018). HDAC3 Mediates Cardioprotection of Remifentanil Postconditioning by Targeting GSK-3beta in H9c2 Cardiomyocytes in Hypoxia/Reoxygenation Injury. Shock *50*, 240–247. https://doi.org/10.1097/SHK.0000000000001008.
29. Jamieson, C., Sharma, M., and Henderson, B.R. (2014). Targeting the beta-catenin nuclear transport pathway in cancer. Semin. Cancer Biol. *27*, 20–29. https://doi.org/10.1016/j.semcancer.2014.04.012.
30. Burgy, O., and Königshoff, M. (2018). The WNT signaling pathways in wound healing and fibrosis. Matrix Biol. *68–69*, 67–80. https://doi.org/10.1016/j.matbio.2018.03.017.
31. Hsieh, C.H., Cheng, L.H., Hsu, H.H., Ho, T.J., Tu, C.C., Lin, Y.M., Chen, M.C., Tsai, F.J., Hsieh, Y.L., and Huang, C.Y. (2013). Apicidin-resistant HA22T hepatocellular carcinoma cells strongly activated the Wnt/beta-catenin signaling pathway and MMP-2 expression via the IGF-IR/PI3K/Akt signaling pathway enhancing cell metastatic effect. Biosci. Biotechnol. Biochem. *77*, 2397–2404. https://doi.org/10.1271/bbb.130503.
32. Hu, H.H., Cao, G., Wu, X.Q., Vaziri, N.D., and Zhao, Y.Y. (2020). Wnt signaling pathway in aging-related tissue fibrosis and therapies. Ageing Res. Rev. *60*, 101063. https://doi.org/10.1016/j.arr.2020.101063.
33. Vilchez, V., Turcios, L., Marti, F., and Gedaly, R. (2016). Targeting Wnt/beta-catenin pathway in hepatocellular carcinoma treatment. World J. Gastroenterol. *22*, 823–832. https://doi.org/10.3748/wjg.v22.i2.823.
34. Jensen, E.C. (2013). Quantitative analysis of histological staining and fluorescence using ImageJ. Anat. Rec. *296*, 378–381. https://doi.org/10.1002/ar.22641.
35. Suetomi, T., Willeford, A., Brand, C.S., Cho, Y., Ross, R.S., Miyamoto, S., and Brown, J.H. (2018). Inflammation and NLRP3 Inflammasome Activation Initiated in Response to Pressure Overload by Ca(2+)/Calmodulin-Dependent Protein Kinase II delta Signaling in Cardiomyocytes Are Essential for Adverse Cardiac Remodeling. Circulation *138*, 2530–2544. https://doi.org/10.1161/CIRCULATIONAHA.118.034621.

STAR★METHODS

KEY RESOURCES TABLE

REAGENT or RESOURCE	SOURCE	IDENTIFIER
Antibodies		
Anti-Rabbit FN-1	Proteintech	Cat#15613-1-AP; RRID: AB_2105691
Anti- Rabbit NET-1	Proteintech	Cat#28180-1-AP; RRID: AB_2881082
Anti- Rabbit α-SMA	Proteintech	Cat#55135-1-AP; RRID: AB_10949628
Anti-Mouse GAPDH	Proteintech	Cat#60004-1-Ig; RRID: AB_2107436
Anti- Rabbit Collagen I	Wanleibio	Cat#WL0088
Anti- Rabbit β-Catenin	Proteintech	Cat#51067-2-AP; RRID: AB_206128
Anti- Rabbit GSK3β	Proteintech	Cat#22104-I-AP; RRID: AB_2878997
Anti- Rabbit GSK3β-Ser9	Proteintech	Cat#67588-7-Ig;
Anti- Rabbit Phospho-Smad3	Abclonal	Cat#0727-AP; RRID: AB_2863813
Anti- Rabbit GSK3β-Ser389	Proteintech	Cat#14850-I-AP; RRID: AB_2878085
Chemicals, peptides, and recombinant proteins		
TRIzol Reagent	Thermo Fisher	Cat# 15596026
Opti-MEM Medium	Gibco	Cat# 31985-062
Phosphate Buffered Saline (PBS)	Solarbio	Cat# P1010
FBS	Corning	Cat# 35-081-CV
SDS	Biofroxx	Cat# 3250KG001
Lipofectamine 2000	Thermo Fisher	Cat#11668019
DMEM	Thermo Fisher	Cat#C11965500BT
Cell-Light Edu Apollo567 *In Vitro* Kit	Ribobio	Cat# C10310-1
DAPI	Beyotime	Cat# C1005
RIPA Lysis	Beyotime	Cat# P0013K
Triton-X100	Beyotime	Cat# AF1504
Hydroxyproline(HYP) assay kit	Jiancheng Bioengineering Institute	Cat# A030-1-1
TGF-β1	Proteintech	Cat# HZ-101
siRNA-NET1	Ribobio	Cat# siG1909050948390672
siRNA-GSK3β	Ribobio	Cat# siG13614133954
siRNA-β-Catenin	Ribobio	Cat# siCtnnb112387
pcDNA3.1+NET1(overexpression-NET1)	AIYOU BIOSCIENCES	Aiyou-K19032219
Experimental models: Organisms/strains		
Mouse: C57BL/6	Experimental Animal Center of the Second Affiliated Hospital of Harbin Medical University.	N/A
CRISPR/Cas9 NET1 knockout (KO) model C57BL/6	www.cyagen.com.cn (Santa clara, USA)	NTCMK170505CAQ02
Oligonucleotides		
Mmu-Col 1α1-F AAGAAGACATCCCTGAAGTCA	Invitrogen	N/A
Mmu-Col 1α1-R TTGTGGCAGATACAGATCAAG	Invitrogen	N/A
Mmu-Col 3α1-F CTGTAACATGGAAACTGGGGAAA	Invitrogen	N/A
Mmu-Col 3α1-R CCATAGCTGAACTGAAAACCACC	Invitrogen	N/A
Mmu-GAPDH-F AAGAAGGTGGCCTGCGCAGGC	Invitrogen	N/A
Mmu-GAPDH-R TCCACCACCCGGTTGTTGCGC	Invitrogen	N/A
Mmu-NET1-F GAGCCAAGCAATAAAAGAGTTCG	Invitrogen	N/A

(*Continued on next page*)

Continued

REAGENT or RESOURCE	SOURCE	IDENTIFIER
Mmu-NET1-R TGGGACTGTTGACCTGCTAGA	Invitrogen	N/A
Mmu-β-catenin-F ATGGAGCCGGACAGAAAAGC	Invitrogen	N/A
Mmu-β-catenin-R TGGGAGGTGTCAACATCTTCTT	Invitrogen	N/A
Software and algorithms		
Prism	Graph Pad	http://www.graphpad.com
ImageJ	National Institutes of Health	https://imagej.nih.gov/ij/index.html

RESOURCE AVAILABILITY

Lead contact

Further information and requests for resources and reagents should be directed to and will be fulfilled by the lead contact, Xuelian Li (lixuelian@hrbmu.edu.cn).

Materials availability

This study did not generate new unique reagents.

Data and code availability

- Data reported in this paper will be shared by the lead contact upon request.
- This paper does not report original code.
- Any additional information required to reanalyze the data reported in this paper is available from the lead contact upon request.

EXPERIMENTAL MODEL AND STUDY PARTICIPANT DETAILS

Study approval

All experimental procedures performed in studies involving animal participants were approved by the Institutional Animal Care and Use Committee of Harbin Medical University, China and the Guide for the Care and Use of Laboratory Animals, published by the US National Institutes of Health (NIH Publication No. 85–23, revised 1996).

Mouse model of myocardial infarction

Male C57BL/6 mice weighing 20-25 g were purchased from the Experimental Animal Center of the Second Affiliated Hospital of Harbin Medical University. The NET1 knockout mouse (KO) model (C57BL/6) by CRISPR/Cas9-mediated genome engineering was established from cyagen (Santa clara, USA). All animal protocols used in the experiments were approved by the Institutional Animal Care and Use Committee of Harbin Medical University. Mice were anesthetized with 1% pentobarbital sodium via intraperitoneal injection and were ventilated. Following left thoracotomy and pericardiotomy, the left anterior descending coronary artery was ligated approximately 1-2 mm below the left atrial appendage with a 7-0 surgical ligature. The heart was immediately reset, and the chest was closed. In the sham group, the coronary arteries were threaded without ligation.

Cardiac fibroblast isolation and culture

Cardiac fibroblasts were isolated from neonatal mice (1-3 days old). After cleaning the mice with 75% ethanol, the hearts were harvested and placed in a petri dish containing phosphate-buffered saline (PBS). The hearts were enzymatically digested in a 5 mL solution containing 60% D'hanks and 40% trypsin (Beyotime, Shanghai, China) at 4°C with agitation for 8-12 h. Thereafter, type II collagenase was added. The digestion was repeated thrice until tissues were completely digested. After collecting the supernatant and centrifuging at 4°C for 5 min, the cell pellet was added to DMEM containing 10% FBS (Biological Industries, Israel) and pipetted. The cells were placed in a constant-temperature cell culture box at 37°C and then spun down to isolate cardiomyocytes and cardiac fibroblasts after 1.5 h and were cultured for a further 48 h.

METHOD DETAILS

Western blot

The proteins were extracted with a RIPA buffer (Beyotime, Shanghai, China) complete protease inhibitor mixture. A bicinchoninic acid protein assay kit (Beyotime, Shanghai, China) was used to measure the protein concentration in the samples. Each sample underwent 5%–15% SDS-PAGE separation before being transferred to nitrocellulose membranes (Merck Millipore, MA, USA). The protein was first cultured with 5% non-fat dry milk for 1.5 hours, followed by an overnight incubation at 4°C with primary antibodies against NET1 (Proteintech, 28180-1-AP),

alpha-smooth muscle actin (α-SMA; Proteintech, 55135-1-AP), fibronectin 1 (FN-1, Proteintech, USA), collagen I (Wanleibio, WL0088), β-catenin (Proteintech, 51067-2-AP), GAPDH (Proteintech, 60004-1-Ig), α-actinin (Proteintech, USA), glycogen synthase kinase-3β (GSK3β; Proteintech, 22104-I-AP), GSK3β- serine 9 (S9) (Proteintech, 67588-7-Ig), and GSK3β- serine 389 (S389) (Proteintech, 14850-I-AP). Densitometric analysis of the bands was performed using Odyssey3.0 Software, and all bands were normalized to GAPDH levels as a control for the equal loading of samples in the total protein extracts.

Quantitative reverse transcription-PCR

Total RNA was extracted from cardiac fibroblasts using the TRIzol method. Total RNA (5 μg) was reverse transcribed using the High-Capacity cDNA Reverse Transcription Kit (Applied Biosystems, USA), and mRNA expression was determined using SYBR Green reagent (Applied Biosystems, USA) in an ABI 7500 Real-Time polymerase chain reaction (PCR) System. The PCR primers were designed and synthesized by Invitrogen. Target genes were applied as internal controls using GAPDH. Relative gene expression data were analyzed using the $2^{-\Delta\Delta Ct}$ method.

Immunofluorescence assay

Cardiac fibroblasts were cultivated in 24-well plates. After fixation with 4% paraformaldehyde for 30 min, cells were permeabilized with 0.4% Triton X-100 (Beyotime, Shanghai, China) for 30 min. The cells were then treated overnight with antibodies at 4°C after being blocked with 50% bovine serum albumin (BSA) for 1 h. The next day, the cells were washed thoroughly and incubated at room temperature for 1 h with Alexa Fluor 488-conjugated antibody or Alexa Fluor 594-conjugated antibody (Abcam, USA). After washing, the nuclei were stained with DAPI (Beyotime, Shanghai, China). The fluorescence signals were observed using a confocal laser scanning microscope (Nikon 80i, Nikon Corporation, Tokyo, Japan). α-SMA fluorescence intensity in fibroblasts was analyzed.[34,35] Fluorescence was converted into pixels using the ImageJ software, and the integrated density (area × mean grey value), as an indirect assessment of α-SMA expression, was calculated. α-SMA was expressed as the integrated density.

EdU assay

Cells were incubated in 24-well plates with EdU solution (Ribobio, Guangzhou, China) at 37°C for 12 h. The cells were incubated in Apollo staining solution at room temperature for 30 minutes without exposure to light after being fixed with 4% paraformaldehyde at room temperature for 30 min and incubated in glycine solution for 5 min. Nuclei were stained with DAPI for 6 min. Images of EdU and DAPI fluorescence in cells were captured using a fluorescence microscope.

Masson staining

Cardiac tissues were rapidly removed after the mice were sacrificed, fixed in 4% paraformaldehyde, embedded in paraffin, and sectioned into 5 μm-thick slices. Paraffin-embedded slices (4 μm) were stained with Masson's trichrome stain. Morphological changes in cardiac tissue were examined under a microscope.

Wound healing assay

Cells were cultivated in 6-well plates. We used 10 μL pipette tips to scratch the cell monolayer in a straight line, and then, the cells were washed twice with PBS. Wound width was imaged under a light microscope at 0, 24, and 48 h after transfection.

Plasmid transfection and TGF-β1 administration

Cells were cultured in a serum-free medium and treated with TGF-β1 (10 ng/mL). Next, NET1-overexpressing plasmid and GSK3β-siRNA (Ribobio, Guangzhou, China) were transfected into cardiac fibroblasts using Lipofectamine 2000 (Invitrogen, CA, USA). After 6-8 h of transfection, the medium was replaced with a fresh standard culture medium.

Transmission electron microscopy

Cardiac tissues were separated into a volume of approximately 1 mm^3 and fixed with 2.5% glutaraldehyde. They were rinsed with 0.1 mol/L phosphoric acid rinsing solution three times and fixed with a 1% osmic acid fixative solution for 3 h. The tissues were then dehydrated once with ethanol and three times at 20 min each with acetone at room temperature. An ultrathin slicer was used for slicing, and the sections were electron-stained and observed under an electron microscope.

MTT assay

Cells were cultured in 96-well plates at 1000-10000 cells per well in 200 μL culture medium. After treatment, the cells were incubated with the MTT solution (5 mg/mL, 20 μL) for 4 h. After adding DMSO (150 μL) to each well, absorbance was measured at 490 nm and 570 nm using a microplate reader.

Co-immunoprecipitation assay

After the cells were lysed, 20 μL of the cell lysis supernatant was added to the loading buffer and boiled for 5 min as the input group. Subsequently, 50 μL of magnetic beads and 200-400 μL PBS were added and mixed gently. The EP tube was placed into the magnetic rack, and the supernatant was discarded; this was completed twice. The diluted antibody was then added to the magnetic beads, spun at room temperature for 30 min for magnetic separation, and then washed with PBS. An antigen-containing sample was added to the EP tube and gently mixed. Finally, the magnetic separation mixture was used, and the supernatant was discarded. The mixture was washed 2-3 times with PBS (magnetic separation was performed between each wash), and the supernatant was discarded. The complex was resuspended in 400 μL PBS and transferred to a new tube. The samples were boiled for 5 min after elution.

Hydroxyproline (HYP) assay

The cell culture fluid was collected and analyzed using a hydroxyproline assay kit (Jiancheng Bioengineering Institute, Nanjing, China). Using a microplate reader with a 550 nm wavelength, the samples' absorbance was recorded. The findings were determined after a standard curve was drawn.

QUANTIFICATION AND STATISTICAL ANALYSIS

Correlation analysis

A total of 73 samples from seven datasets were used in this study, as described in Table S1. The probe-set identifiers were annotated to Entrez gene IDs or gene symbols using the matching platform information. If multiple probe-sets were annotated to the same gene, their average expression value was defined as expression value of the gene, and probe-sets mapped to multiple genes were excluded. The curated gene sets of signaling pathways for MI were acquired from MSigDB; these included the following: "GOBP_NOTCH_SIGNALING_PATHWAY," "HALLMARK_NOTCH_SIGNALING," "WP_NOTCH_SIGNALING_PATHWAY," "HALLMARK_TGF_BETA_SIGNALING," "BIOCARTA_TGFB_PATHWAY," "BIOCARTA_WNT_PATHWAY," "BIOCARTA_NFKB_PATHWAY," "BIOCARTA_MAPK_PATHWAY," and "WP_MAPK_SIGNALING_PATHWAY." Single sample gene set enrichment analysis was performed with gene set variation analysis to estimate the enrichment score in each sample. Spearman rank correlation analysis was used to analyze the relationship between expression value of NET1 and enrichment scores of signaling pathways. A P value of < 0.05 was considered significant.

Statistical analysis

All data are presented as the mean ± SEM. Between-group comparisons were performed using the Mann Whitney test (non-parametric tests). Meanwhile, multiple-group comparisons were performed using the Kruskal-Wallis test followed by Dunn's multiple comparisons test. GraphPad Prism software (GraphPad 9.0) was used for statistical analyses. $P < 0.05$ was the threshold for statistical significance.